SUPPLEMENTAL DATA

Target Processing and Pertechnetate Purification

Each irradiated target was dissolved in 30% H_2O_2 (2.2 mL). Dissolution of the molybdenum in H_2O_2 is an exothermic reaction but was controlled effectively by cooling the dissolution vessel using compressed air in a way that the reaction temperature would not exceed 25°C. When the exothermic process stopped, the vessel was heated at 90°C for 5 min to decompose unreacted H_2O_2. After cooling to ambient temperature, the solute was basified with 2.5M $(NH_4)_2CO_3$ (2.5 mL) and transferred into another reaction vessel. The crude target solute was passed through a cartridge containing polystyrene-polyethylene glycol (PS-PEG) resin which consists of polystyrene cross-linked with divinylbenzene support and attached to its surface PEG chains (~1.5 g, ABEC (Eichrom), conditioned with 10 mL 2.5M $(NH_4)_2CO_3$). The pertechnetate was retained on the resin, while the rest of the solution, containing ^{100}Mo-molybdate ($[^{100}Mo]MoO_4^{2-}$) and co-produced ^{99}Mo, ^{96}Nb, and ^{97}Nb ionic species, was collected into an empty 20 mL vial for further reprocessing or recycling after radioactivity decay. The mechanism of pertechnetate trapping was not extensively studied, but it was suggested that the low charge to size ratio of pertechnetate results in low Gibbs energy of hydration allowing for hydrophobic interaction with PEG chains (*1*,*2*). In other words, pertechnetate ion is rather large and neutral to partition into PEG at certain conditions and may be selectively eluted afterwards.

The cartridge was washed with 1.0M Na_2CO_3 (3 mL) to remove traces of ammonia and effluent was sent to waste. The product in form of pertechnetate was eluted with water for injection (5 mL) through a series of cation exchange resins, which were divided in two separate cartridges. First cartridge contained 600 mg (1:1) of Diphonix resin (Eichrom) and

50W×8 resin (Eichrom), both strong cation exchange in H^+ form. Diphonix resin is functionalized with diphosphonic and sulphonic acid group residues while 50W×8 resin contains sulfonic acid groups only. Sulfonic acid groups retain strong base polyvalent cations, alkaline earth and transition metals. Diphosphonic acid groups have preference for trivalent and higher valence cation retention. Second cartridge contained 600 mg of Amberlite IRC86 (Dow Chemical), weak cation-exchange resin in H^+ form. This weakly acidic dealkalyzation/water-softening resin served to neutralize product solution to a desired pH by removing ammonium and sodium ions. All used cation-exchange resins have no affinity to pertechnetate, which is an anionic form of technetium. Both cartridges were preconditioned with high-purity water (40 mL each). The pertechnetate was collected into a vial containing 4M NaCl (0.2 mL, final concentration NaCl 0.9%).

All manipulations were performed using an in-house built automated processing apparatus, which combines target dissolution and purification of the pertechnetate in a single process. Equipment was remotely controlled by Lookout software (National Instruments).

References:

1. Rogers RD, Bond AH, Griffin ST, Horwitz EP. New technologies for metal ion separations: aqueous biphasic extraction chromatography (ABEC). Part I Uptake of pertechnetate. *Solvent Extr Ion Exch*. 1996;14:919–946.

2. Harvey J, Gula M. Separation, concentration, and immobilization of technetium and iodine from alkaline supernate waste. DOE SciTech Connect technical report. 1998. doi:10.2172/2144. Retrieved from http://www.osti.gov/scitech/servlets/purl/2144

Calibration of gamma-ray detector

The gamma-ray spectrometry system consisted of a GMX series GAMMA-X High-Purity Germanium (HPGe) coaxial photon detector (model GMX30P4-70-SMN, ORTEC) connected to a DSPEC Jr. 2.0 (ORTEC) multichannel analyzer and controlled by Maestro 6.0 software (ORTEC). Measured energy resolution was 1.98 keV at full width at half maximum (FWHM) for ^{60}Co peak at 1332 keV. Two-point energy calibration was performed using 2 photopeaks with known energies: 122 keV of ^{57}Co and 1332 keV of ^{60}Co. Efficiency of an HPGe detector is dependent on the energy of measured gamma-rays and was determined using a set of standard sealed coin-shaped radioactivity sources, namely ^{133}Ba, ^{109}Cd, ^{57}Co, ^{60}Co, ^{137}Cs, ^{54}Mn, and ^{22}Na (Eckert & Ziegler). For this, the spectra were acquired at a fixed distance of 25 cm from the detector for 3600 sec detector live time. The net counts corresponding to the integration area of each characteristic gamma-ray peaks were decay corrected to the start of acquisition. Detector efficiency was calculated as a ratio of measured radioactivity of each standard divided by its nominal radioactivity at start of acquisition and expressed in percent. Calibration curve was built over energy range 0-2000 keV using obtained detector efficiency values. The data were fitted using two separate equations: a quadratic function for the energies below 280 keV and power function for the energies over 280 keV (Supplemental Figure 1). Fitted function equations were used to correct for detector efficiency when quantifying produced radioisotopes.

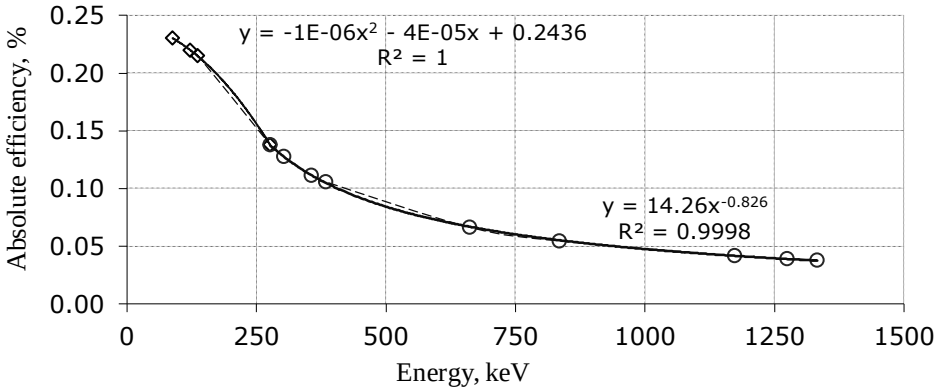

SUPPLEMENTAL FIGURE 1. Efficiency calibration curve for the HPGe detector.

Quantitative Determination of Radionuclidic/Radioisotopic Impurities

A gamma-ray spectrum of a test sample in a standardized configuration was acquired using a calibrated High-Purity Germanium (HPGe) detector (the calibration procedure is described above) keeping the detector dead time below 5% (dilutions were employed if required) and analyzed for the presence of characteristic photopeaks of Tc, Mo, and Nb isotopes (Supplemental Table 1). Blank measurement was taken to account for background radioactivity (subtracted from the sample spectrum). Photopeak integrations were performed using dedicated software (Maestro, ORTEC) accounting for Compton background.

The net counts (area) under the integrated isotope energy peaks were corrected for relative gamma intensity (for each associated gamma-ray peak), detector dead time, detector efficiency (using the efficiency calibration curve equation obtained as described above), and radioactivity decay and expressed in Bq. Percentage of each radioisotope radioactivity in the sample was calculated as the radioactivity for the isotope of interest (Bq) divided by total radioactivity in the sample (the sum of the radioactivities of all detected isotopes (Bq).

SUPPLEMENTAL TABLE 1. Physical properties used to quantify the radioactivity due to each nuclide (*1*).

Nuclide	Half-life $T_{1/2}$, h	Gamma-ray energy E_γ, keV	Relative intensity of gamma-ray I_γ, %
^{99m}Tc	6.015	140.511	89.06
^{97m}Tc	2184	96.5	0.32
^{96}Tc	102.7	812.54	82
^{96m}Tc	0.858	778.22	1.9
^{95}Tc	20	765.789	93.8
^{95m}Tc	1464	582.082	30.0
^{94}Tc	4.9	702.67	99.6
^{94m}Tc	0.867	1868.68	5.7
^{93}Tc	2.75	1362.94	66.2
^{93m}Tc	0.725	391.83	58.3
^{99}Mo	65.94	739.500	12.13
^{99}Mo	65.94	140.511	4.52
^{97}Nb	1.20	657.94	58.0
^{96}Nb	23.55	568.871	98.23

(*1*) Brookhaven National Laboratory National Nuclear Data Center, Nuclear structure and decay data NuDat 2.5 (2011), http://www.nndc.bnl.gov/nudat2/

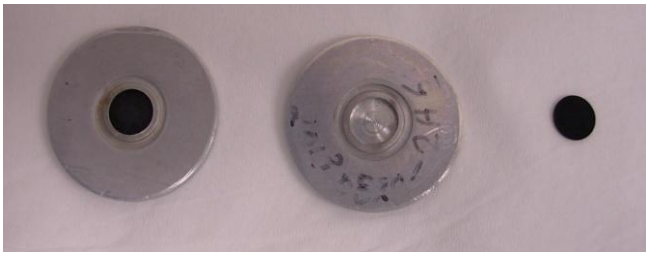

SUPPLEMENTAL FIGURE 2. Undissolved part of ^{100}Mo pellet detached from aluminium support after decay of irradiated target.

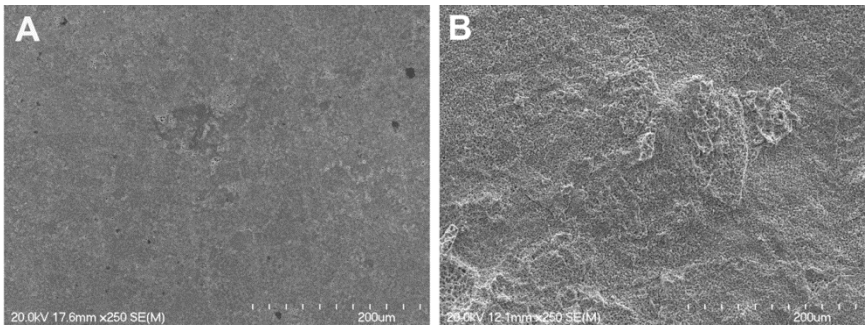

SUPPLEMENTAL FIGURE 3. Typical surface of ^{100}Mo target before irradiation (A) and after dissolution (B) as seen with scanning electron microscopy (resolution 200 μm).

SUPPLEMENTAL TABLE 2. Potential dose from each Tc isotope if injected individually.

Organ/Tissue	Tc-93	Tc-94m	Tc-94	Tc-95m	Tc-95	Tc-96m	Tc-96	Tc-97m	Tc-99m
Adrenals	1.93E-02	1.33E-02	4.64E-02	8.21E-02	3.47E-02	3.87E-04	2.10E-01	2.13E-02	3.28E-03
Brain	8.96E-03	8.86E-03	2.43E-02	5.06E-02	1.95E-02	2.91E-04	1.22E-01	2.12E-02	1.93E-03
Breasts	9.75E-03	9.04E-03	2.42E-02	4.65E-02	1.88E-02	2.90E-04	1.16E-01	2.10E-02	1.66E-03
Gallbladder Wall	4.03E-02	1.79E-02	8.05E-02	1.19E-01	5.88E-02	4.88E-04	3.21E-01	2.15E-02	5.87E-03
Lower Large Intestine Wall	1.17E-01	2.63E-02	1.56E-01	5.90E-01	2.02E-01	8.14E-04	1.22E+00	8.71E-01	2.04E-02
Small Intestine	9.54E-02	1.22E-01	1.55E-01	2.15E-01	1.10E-01	4.13E-03	5.80E-01	7.13E-02	1.55E-02
Stomach Wall	6.42E-02	1.41E-01	1.25E-01	1.16E-01	6.45E-02	4.93E-03	3.12E-01	4.98E-02	1.12E-02
Upper Large Intestine Wall	1.71E-01	8.14E-02	2.49E-01	3.22E-01	1.80E-01	2.78E-03	8.21E-01	3.10E-01	2.73E-02
Heart Wall	1.60E-02	1.22E-02	4.04E-02	7.45E-02	3.06E-02	3.64E-04	1.89E-01	2.12E-02	2.85E-03
Kidneys	2.48E-02	1.42E-02	5.32E-02	8.80E-02	3.96E-02	4.07E-04	2.31E-01	2.13E-02	3.70E-03
Liver	2.08E-02	1.27E-02	4.71E-02	8.13E-02	3.58E-02	3.74E-04	2.11E-01	2.13E-02	3.29E-03
Lungs	1.27E-02	1.05E-02	3.23E-02	6.23E-02	2.51E-02	3.31E-04	1.54E-01	2.14E-02	2.40E-03
Muscle	1.93E-02	1.18E-02	4.20E-02	7.85E-02	3.34E-02	3.56E-04	2.02E-01	2.13E-02	2.93E-03
Ovaries	6.95E-02	2.22E-02	1.22E-01	2.38E-01	1.09E-01	6.15E-04	6.52E-01	2.48E-02	8.72E-03
Pancreas	2.89E-02	1.95E-02	6.64E-02	9.58E-02	4.43E-02	5.34E-04	2.52E-01	2.13E-02	4.61E-03
Red Marrow	2.19E-02	1.11E-02	4.80E-02	9.05E-02	3.92E-02	3.56E-04	2.40E-01	1.41E-02	3.22E-03
Osteogenic Cells	1.95E-02	1.43E-02	4.52E-02	8.83E-02	4.23E-02	3.14E-03	2.26E-01	2.22E-02	7.16E-03
Skin	1.09E-02	8.91E-03	2.45E-02	4.67E-02	1.93E-02	2.76E-04	1.19E-01	2.04E-02	1.69E-03
Spleen	2.26E-02	1.57E-02	5.20E-02	8.20E-02	3.64E-02	4.40E-04	2.13E-01	2.13E-02	3.63E-03
Testes	1.82E-02	1.09E-02	3.97E-02	8.28E-02	3.30E-02	3.33E-04	2.08E-01	2.11E-02	2.70E-03
Thymus	1.23E-02	1.04E-02	3.26E-02	6.49E-02	2.57E-02	3.25E-04	1.61E-01	2.12E-02	2.33E-03
Thyroid	8.21E-02	3.26E-01	1.60E-01	1.34E-01	7.71E-02	1.25E-02	3.06E-01	1.72E-01	2.16E-02
Urinary Bladder Wall	1.08E-01	8.86E-02	1.71E-01	3.18E-01	1.18E-01	2.99E-03	6.58E-01	2.35E-01	1.65E-02
Uterus	5.49E-02	2.19E-02	1.04E-01	1.75E-01	7.82E-02	5.85E-04	4.53E-01	2.16E-02	7.50E-03
Total Body	2.01E-02	1.33E-02	4.31E-02	8.02E-02	3.41E-02	4.13E-04	2.05E-01	2.49E-02	3.27E-03
Effective Dose Equivalent	**5.94E-02**	**4.73E-02**	**1.01E-01**	**1.89E-01**	**8.28E-02**	**1.69E-03**	**4.68E-01**	**1.12E-01**	**9.42E-03**
Effective Dose	**5.61E-02**	**5.08E-02**	**9.62E-02**	**1.87E-01**	**7.77E-02**	**1.79E-03**	**4.46E-01**	**1.45E-01**	**9.26E-03**